POAC'17
Busan, KOREA

Proceedings of the 24th International Conference on
Port and Ocean Engineering under Arctic Conditions
June 11-16, 2017, Busan, Korea

Concrete-Ice Abrasion Laboratory Experiments

Guzel Shamsutdinova[1], Max A.N. Hendriks[1,2], Stefan Jacobsen[1]
[1] Norwegian University of Science and Technology, Trondheim, Norway
[2] Delft University of Technology, Delft, Netherlands

ABSTRACT

Concrete-ice abrasion is a concrete surface degradation mechanism due to ice-structure interaction. The topic is especially relevant for concrete gravity-based structures in the Arctic offshore.

Experiments have become the main evaluation method for concrete durability under ice abrasion. The paper presents concrete-ice abrasion experiment between sawn concrete surface (cubic compressive strength is 90 MPa) and unidirectional fresh water ice. The experiment included two experimental conditions, with varied temperature of the concrete surface.

Results demonstrate the load cells response, coefficient of friction and abrasion depth. Based on our results and observations we identified wet and dry abrasion types. The first type caused most damage, whereas second one caused minor damage.

KEY WORDS: Concrete; Ice; Abrasion; Experiment.

INTRODUCTION

The concrete-ice abrasion process has been studied for the last 30 years, and has been defined as the surface degradation of concrete structures due to interaction with drifting ice floes. Several research groups have studied this topic through laboratory experiments (Huovinen, 1993, Bekker et al., 2011, Hanada et al., 1996, Fiorio, 2005, Møen et al., 2015, Tijsen et al., 2015) and field observations (Itoh et al., 1996, Huovinen, 1993). Hara et al. (Hara et al., 1995) recommended the concrete-ice sliding abrasion test, during evaluation of various test methods of concrete-ice abrasion resistance. And so far most experimental work has been based on the sliding interaction between ice and concrete, whether ice on concrete (Fiorio, 2005, Møen et al., 2015, Saeki et al., 1986) or concrete on ice (Hoff, 1989, Bekker et al., 2011, Tijsen et al., 2015, Itoh et al., 1988).

Our experimental method is based on the sliding of an ice sample along a fixed concrete sample, and controls exposure, measures relevant response parameters during concrete-ice interaction including concrete-ice abrasion with a non-contact laser scanner.

EXPERIMENT

This experimental studying included the abrasion machine for simulation of concrete-ice abrasion, and a laser scanner for further measuring of abrasion wear. The experimental equipment is described below together with the employed concrete and ice.

Abrasion Machine

The abrasion machine (Figure 1(a)) simulated concrete-ice abrasion according to the principle in Figure 1(b), with a sliding ice specimen along a fixed concrete sample.

The machine makes the ice sample holder move in repeated sliding movements in a horizontal direction, with the average velocity 0.16 m/s. The piston (Figure 1(a), no 3) continuously pushes the ice sample against the concrete surface with 1 MPa load. A feedback system keeps the loading as constant as possible during the test while moving back and forth. The temperature in the concrete-ice abrasion lab is kept at temperature of −10 °C.

The concrete sample temperature control goes through an aluminum heating plate that is below the concrete sample (Figure 1(a), no 7). The plate is connected to a controlled temperature liquid (alcohol) circulator. This means that the temperature of the concrete surface in the concrete-ice abrasion zone can be adjusted. The temperature of the concrete surface in the contact zone was measured with an infrared scanner. More detailed information about the components of the abrasion machine is given in (Shamsutdinova et al., 2015).

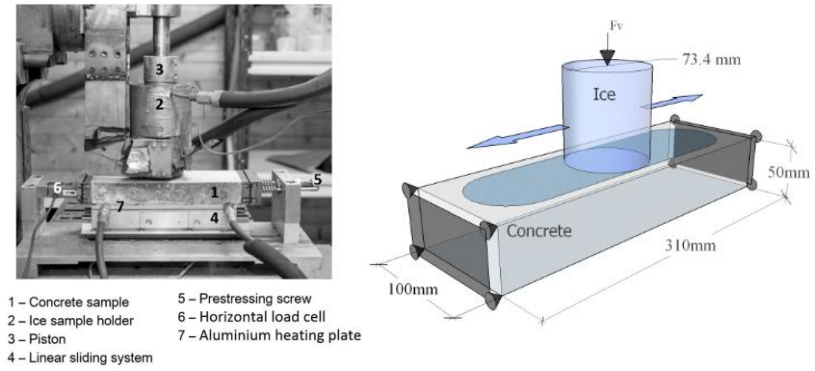

(a) (b)

Figure 1. The concrete-ice abrasion machine: (a) photo, (b) principal scheme.

Laser Scanner

Recently, we developed a non-contact Laser Scanning method (Figure 2(a)) to measure concrete-ice abrasion. It allows scanning of the concrete surface with accuracy 10 μm in reasonable time. The laser moves continuously along the sample according to a predefined "snaking" path. The measuring point distance is approximately 50 μm in the Y direction, and the step size in the X direction is 1 mm (Figure 2(b)). The measured data is transformed to a matrix of surface heights, with 1900x300 points.

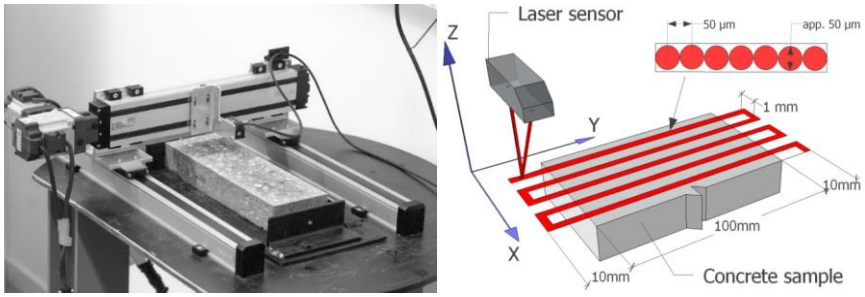

(a) (b)

Figure 2. Laser scanner: (a) photo; (b) simplified schematic of measurement process (not to scale).

Ice

Our abrasion machine is designed for fresh-water cylindrical ice samples. We used unidirectionally grown ice made from tap water, which can easily be reproduced in other laboratories.

An ice mould made of Polyoxymethylene (POM) 13.3 mm thick and 370 mm high (Figure 3(a)) and covered with thermo isolation on the sides and the bottom is filled with tap water and put in a freezer at −20 °C for 48-72 hours. The freezing of the water starts at the top of the mould, but later it also takes place from the bottom (Figure 3(b,c)). The upper part of the ice sample is transparent (unidirectionally grown ice) with very few air voids. The lower part of the ice sample contains a lot of air voids and unfrozen water. The ice sample is cut in two, and only the upper part is used for the test (Figure3(d).

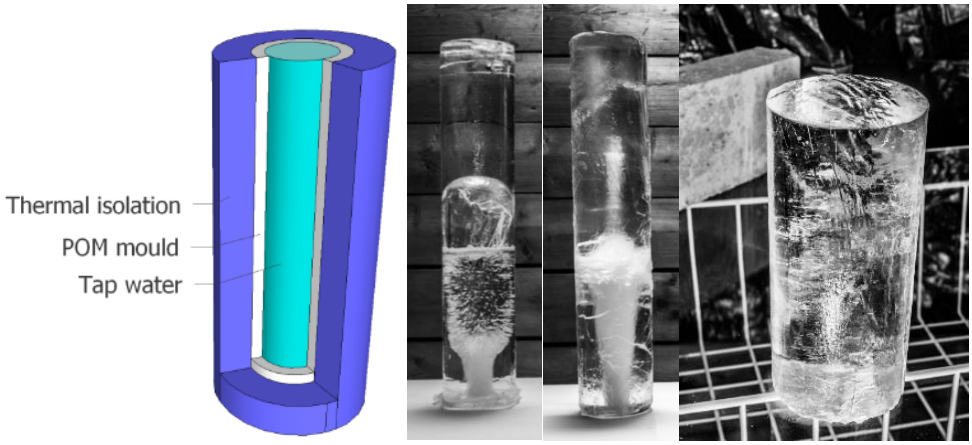

(a) (b) (c) (d)

Figure 3. Schematic of ice production: (a) ice mould with isolation; (b) ice sample after 48 hours; (c) ice sample after 72 hours; (d) ice sample for the test.

Concrete

The tests were carried out with two concrete samples made of Norcem Anlegg (CEM I) cement (with 2% Elkem silica fume substitution) with fine aggregate (Årdal sand, 0-8 mm grain size) and coarse aggregate (Årdal, 8-16 mm grain size). The mix was made with the following proportion: W/(C+2S)=0.42, where W, C and S are the weight of water, cement and silica fume powder, respectively. The cement paste volume was 29.5%. Superplasticizing additive

Dynamon SX-23 from Mapei was used to achieve target workability.

The 28-day cube compressive strength of the concrete was 90 MPa. Samples were cured in water at +20°C for 11 months, reaching 110 MPa cube compressive strength by the start of the test.

Experimental Conditions

As was said above, the tests were performed in the abrasion laboratory at air temperature -10°C. The ice pressure was 1 MPa. The average sliding velocity was 0.16 m/s. The experiment was performed on two concrete samples with varied temperature of concrete surface in the sliding zone. The temperature variation went through aluminum heating plate (Figure 1(a), no 7). Sample 1 had surface temperature +2°C at the start of the test, and Sample 2 had surface temperature -4°C at the start of the test. Both samples had sawn concrete surface.

RESULTS

The data acquisition system logged horizontal and vertical load cells responses during the test at 500 Hz frequency. The absolute coefficient of friction (COF) is plotted in Figure 4 for two samples. The highest COF corresponds to the turning points of the ice specimen where the ice sample makes a full stop. We distinguished the coefficient of kinetic friction during sliding interaction, and the coefficient of static at the turning points. The coefficient of kinetic friction varied in the range 0 to 0.02, whereas the coefficient of static friction varied from 0.05 to 0.10. Figure 4 shows that Sample 2, with concrete surface temperature -4°C, resulted in the smallest COF.

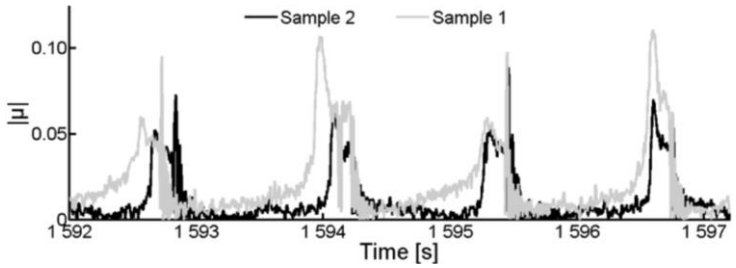

Figure 4. Coefficient of friction for two tested samples.

Figure 5 demonstrates the result of surface scanning before and after 4 km of abrasion test. On the left side, before the test, the concrete surface has diamond saw blade traces. On the right side, after 4 km of abrasion test, the concrete surface became rougher.

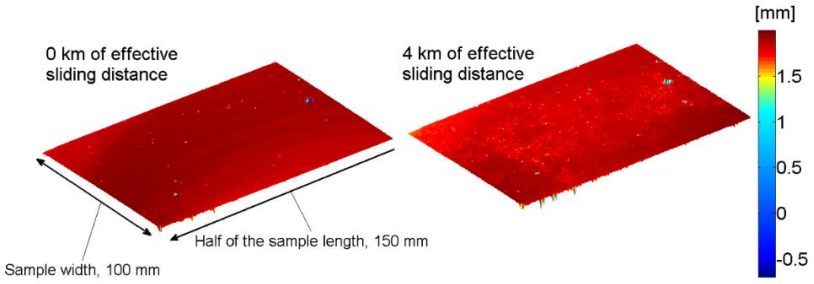

Figure 5. Scans of Sample 1, before abrasion test and after 4 km of abrasion test (half of the scanned sample).

Based on the surface measurements, abrasion was found as difference between the unabraded rim of the concrete sample and an abraded central band of 10 mm wide as done with mechanical measurements in (Møen et al., 2015). However, a much higher number of data points was collected with the laser scanner, so the calculation here was done for each millimeter of concrete sample length. Figure 6 shows the average profile of the abraded central band (10 mm wide) along the sample length, before and after 4 km abrasion test. The difference between dashed and solid lines shows the abrasion. The spikes, in Figure 6, corresponds to the air voids.

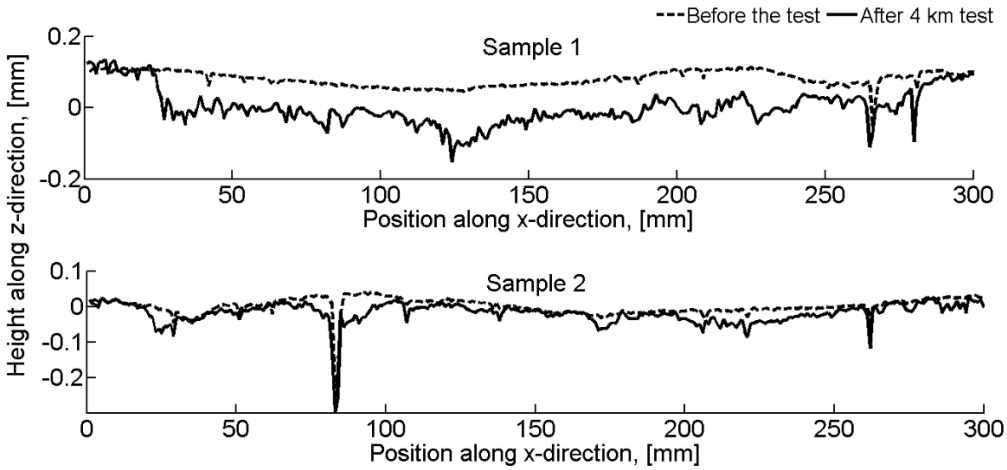

Figure 6. Average profile, of the central abraded band (10 mm wide), of sawn concrete surface along the sample length before and after 4 km abrasion test.

Figure 7 shows average abrasion rate for two samples. The abrasion for Sample 1 with the surface temperature +2°C at the start of the test is much higher than for Sample 2 with the surface temperature -4°C at the start of the test.

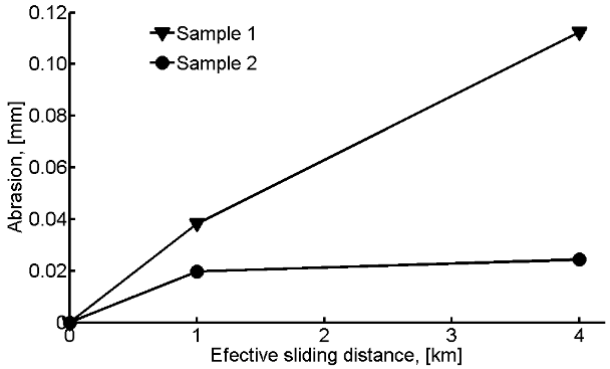

Figure 7. Abrasion of sawn concrete surface from zero to 1 and 4 km.

DISCUSSION AND CONCLUSION

The measured coefficient of kinetic friction is of the same magnitude as test results of other concrete-ice abrasion tests with the same sliding speed (0.16 m/s): 0.00 – 0.01 and 0.06 respectively (Møen et al., 2015, Itoh et al., 1988). Where Itoh et al. used ice pressure 0.2MPa, that is ¼ th of the present test.

The results of abrasion depth were found similar to previous study Møen et al. where concrete samples with cylindrical compressive strength from 72.8 to 147.8 MPa under similar experimental conditions had maximum abrasion rate 0.025 mm/km of effective sliding distance.

Based on our results and observations we distinguished between two types of concrete-ice abrasion exposure: wet and dry, corresponding to Sample 1 and Sample 2 respectively. Dry abrasion happened when the concrete sample had surface temperature -4°C at the start of the test. Ice filled the unevenness on the concrete surface during the first few sliding cycles, and all further sliding was between ice and ice.

In case of wet abrasion, the temperature of the concrete sample surface was +2°C at the start of the test, and it fluctuated between −1.8 and −2.6 °C during the abrasion test. There was a constant thin film of water on the concrete surface, with minor icing spots, during the test.

We conclude that wet abrasion test causes more wear than dry. It means that the concrete surface temperature control system is an important element of the experimental method.

ACKNOWLEDGEMENTS

This research forms part of the DACS (Durable Advanced Concrete Solutions) project. The financial contribution of the Norwegian Research Council is gratefully acknowledged. The DACS project partners are: Kværner AS (project owner), Axion AS (Stalite), AF Gruppen Norge AS, Concrete Structures AS, Mapei AS, Multiconsult AS, NorBetong AS, Norcem AS, NPRA (Statens Vegvesen), Norges Teknisk-Naturvitenskapelige Universitet (NTNU), SINTEF Byggforsk, Skanska Norge AS, Unicon AS and Veidekke Entreprenør AS.

Thanks to Giedrius Zirgulis for the photographs.

REFERENCES

Bekker, A.T., Uvarova, T.E., Pomnikov, E.E., Farafonov, A.E., Prytkov, I.G. & Tyutrin, R.S., 2011. Experimental study of concrete resistance to ice abrasion. Proceedings of the International Offshore and Polar Engineering Conference, pp. 1044-1047.

Fiorio, B., 2005. Wear characterisation and degradation mechanisms of a concrete surface under ice friction. Construction and Building Materials, 19, 366-375.

Hanada, M., Ujihira, M., Hara, F. & Saeki, H., 1996. Abrasion rate of various materials due to the movement of ice sheets. Proceedings of the International Offshore and Polar Engineering Conference, pp. 433-437.

Hara, F., Takahashi, Y. & Saeki, H., 1995. Evaluation of test methods of abrasion by ice movements on the surface of reinforced concrete structures. Concrete Under Severe Conditions Environment and Loading.

Hoff, G.C., 1989. Evaluation of ice abrasion of high-strength lightweight concretes for arctic applications. Proceedings of the International Offshore Mechanics and Arctic Engineering Symposium, pp. 583-590.

Huovinen, S., 1993. Abrasion of concrete structures by ice. Cement and Concrete Research, 23, pp.69-82.

Itoh, Y., Tanaka, Y., Delgado, A. & Saeki, H., 1996. Abrasion depth distribution of a cylindrical concrete structure due to sea ice movement. International Journal of Offshore and Polar Engineering, 6, pp. 144-151.

Itoh, Y., Yoshida, A., Tsuchiya, M., Katoh, K., Sasaki, K. & Saeki, H., 1988. An experimental study on abrasion of concrete due to sea ice. Offshore Technol. Conference, OTC 5687, pp.61-68.

Møen, E., Høiseth, K.V., Leira, B. & Høyland, K.V., 2015. Experimental study of concrete abrasion due to ice friction - Part I: Set-up, ice abrasion vs. material properties and exposure conditions. Cold Regions Science and Technology, 110, pp.183-201.

Saeki, H., Ono, T., Nakazawa, N., Sakai, M. & Tanaka, S., 1986. Coefficient of friction between sea ice and various materials used in offshore structures. Journal of Energy Resources Technology, Transactions of the ASME, 108, pp.65-71.

Shamsutdinova, G., Rike, P.B., Hendriks, M.A.N. & Jacobsen, S., 2015. Concrete ice abrasion rig and wear measurements. Proceedings of the International Conference on Port and Ocean Engineering under Arctic Conditions.

Tijsen, J., Bruneau, S. & Colbourne, B., 2015. Laboratory examination of ice loads and effects on concrete surfaces from bi-axial collision and adhesion events. Proceedings of the International Conference on Port and Ocean Engineering under Arctic Conditions.